MATEC Web of Conferences **14**, 04004 (2014)
DOI: 10.1051/matecconf/20141404004

Oxide-assisted crack growth in hold-time low-cycle-fatigue of single-crystal superalloys

Akane Suzuki[1,a], Yan Gao[1], Don Lipkin[1], Anjali Singhal[1], Matthew Krug[2], Douglas Konitzer[2], Jonathan Almer[3], Tresa Pollock[4], and Bernard Bewlay[1]

[1]GE Global Research, Niskayuna, NY, USA
[2]GE Aviation, Cincinnati, OH, USA
[3]Argonne National Laboratory, Advanced Photon Source, Lemont, IL, USA
[4]University of California, Santa Barbara, Santa Barbara, CA, USA

Abstract. Compressive hold-time low-cycle fatigue is one of the important damage modes in Ni-based superalloy hot-gas path components. In strain controlled LCF, the compressive hold typically degrades fatigue life significantly due to creep relaxation and the resultant generation of tensile stress upon returning to zero strain. Crack initiation typically occurs on the surface, and therefore, the cracks are covered with layers of oxides. Recent finite element modeling based on experimental observations has indicated that the in-plane compressive stress in the alumina layer formed on the surface of the bond coat assists rumpling and, eventually, leads to initiation of cracks. The stress in the oxide layer continues to assist crack extension by pushing the alumina layer along the crack front during the compressive hold. In-situ measurements of the growth strains of alumina were performed using high energy synchrotron X-rays at Argonne National Lab. Specimens of single-crystal superalloys with and without aluminide coatings were statically pre-oxidized to form a layer of alumina at 1093 and 982 °C. For the in-situ synchrotron measurements, the specimens were heated up to the pre-oxidation temperatures with a heater. The alumina layers on both bare and coated specimens show compressive in-plane strains at both temperatures. The oxide strains on the superalloys showed dependency on temperature; on the other hand, the oxide strains in the aluminide coatings were insensitive to temperature. The magnitude of the compressive strains was larger on the superalloys than the ones on the aluminide coatings.

1. Crack growth in hold-time LCF of single-crystal Ni-base superalloys

Resistance to compressive hold-time low-cycle-fatigue (LCF) deformation is one of the important properties required for Ni-base single-crystal superalloys used for internally cooled airfoil components in aircraft engines and land based gas turbines for power generation. Strain controlled compressive hold-time LCF deformation is significantly damaging to the superalloys, because creep deformation during the compressive hold causes the generation of tensile stress upon returning to zero strain. The tensile stress causes initiation and propagation of surface cracks which eventually lead to failure of the material. In a series of interrupted compressive hold-time LCF tests conducted at 1093 °C and 0.35% total strain range using a second generation single-crystal superalloy, René N5 coated with vapor phase aluminide (VPA), it was observed that (i) the surface crack initiation occurred in the early stage (<10%) of the fatigue life and (ii) the surface cracks were covered with an α-Al_2O_3 layer due to the exposure to the air [1]. Figure 1 shows a typical crack observed in the bond coat layer (Fig. 1a) and a crack propagated into the single-crystal superalloy substrate (Fig. 1b) beyond the bond coat layer and the interdiffusion zone.

It has been known that the α-Al_2O_3 layer formed on the surfaces of the bond coats of the superalloys typically have in-plane compressive growth strains due to the volume expansion during oxidation, and that the compressive stress of the oxide layer contributes to the evolution of bond coat rumpling during cyclic oxidation environment [2]. Evans *et al.* [3–5] examined the role of compressive growth strains of the α-Al_2O_3 layer in extension of a crack in isothermal compressive cyclic loading using a finite element model, and predicted that the compressive stress of the α-Al_2O_3 layer causes crack extension by inward extrusion of the α-Al_2O_3 layer along the crack front during compressive loading. The predicted crack growth rate was close to the crack growth rate observed in the interrupted specimens. The model predicted that larger compressive growth strains of the α-Al_2O_3 cause higher crack growth rates in both the bond coat layer and the superalloy substrate.

In-situ measurements of the oxide growth strains have been conducted by Veal *et al.* [6–11] and Almer *et al.* [12] using synchrotron X-rays. The evolution of

[a] Corresponding author: suzukia@ge.com

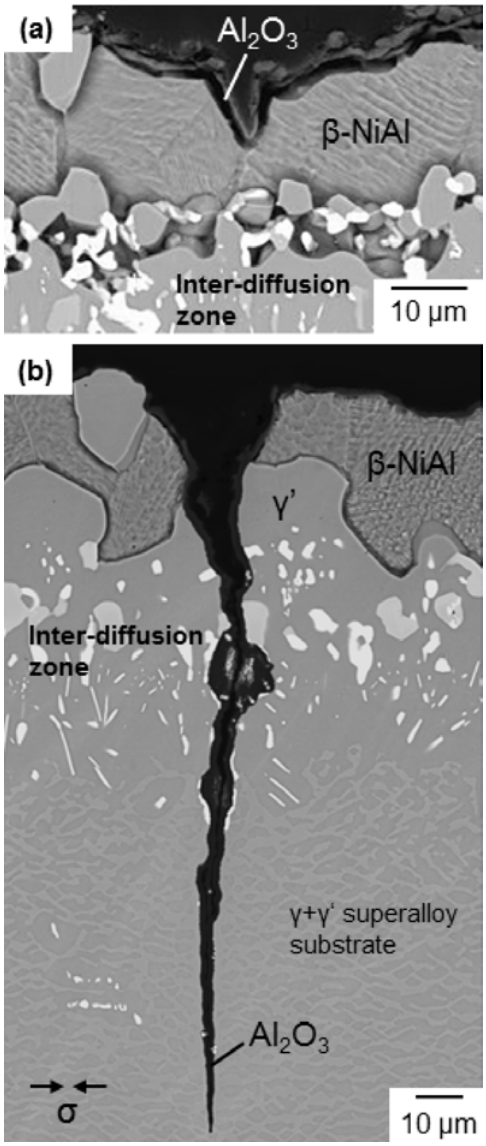

Figure 1. Surface cracks covered with the α-Al_2O_3 layer in (a) the bond coat layer and (b) the superalloy substrate.

the growth strains in the early stage of the oxidation, the creep behaviour of the oxide layer and the effects of alloy chemistry on the oxide growth strains have been investigated using various β-NiAl-based and NiCrAlY alloys. However, there has been a lack of high temperature *in-situ* measurements of the growth strains of the oxide layers formed on single-crystal superalloys and industrial bond coats, except a limited study that used room temperature strain measurements by laser scanning confocal microscopy and thermal expansion data to calculate the oxide growth strains that were generated during prior oxidation at elevated temperatures [13,14].

In this study, *in-situ* measurements of the oxide growth strains were conducted using the oxide layers grown on a single-crystal Ni-base superalloy and a β-NiAl based industrial bond coat. The measurement results and effect of temperature, effect of bond coat composition will be discussed.

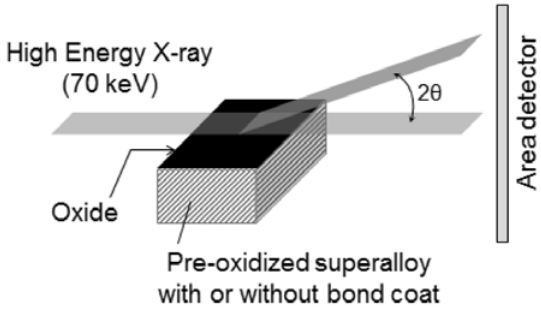

Figure 2. Schematic illustration of the experimental setup.

2. Experimental procedures

The experimental arrangement is illustrated in Fig. 2. In this experiment, a transmission diffraction approach was applied for the oxide growth strain measurements. Compared with the grazing incident diffraction mode used by Veal *et al.* [6–11], the transmission diffraction mode used by Almer *et al.* [12] requires high energy X-rays to penetrate through the material. As the oxide layer thickness is $\sim$1 μm, such high energy X-rays must be from a high brilliance source. The experimental procedure for the transmission diffraction mode is simpler than grazing incident diffraction mode, because it is easier to find the beam center and to align the specimen: both are critical for accurate strain analysis.

The high energy synchrotron X-ray diffraction experiment was performed at Beamline 1-ID-C at Advanced Photon Source, Argonne National Laboratory. A Ni-based René N5 single-crystal superalloy and a β-NiAl-based vapor phase aluminide bond coat were selected for the experiments. The bond coat was deposited on a single-crystal superalloy substrate. Both bare and coated superalloy specimens were machined to 6 mm wide, 10 mm long, 3 mm thick coupons. Prior to the strain measurements, the coupons were isothermally oxidized in air for 68 hours at either 1093 °C or 982 °C to grow oxide layers in advance, to achieve stable state of the oxide growth.

The measurements were conducted at both room temperature and the same high temperatures at which the specimens were pre-oxidized. To heat the pre-oxidized coupons during the *in-situ* measurements, a commercial SiC igniter was used. The surface of the igniter was coated with a protective layer to prevent reaction with the superalloy specimens.

During the *in-situ* measurements, the sample surface temperatures were monitored by a pyrometer mounted above the sample, and were determined based on a lattice parameter of Pt powders placed on the surfaces of the samples. Slurry containing Pt powders and yttria-stabilized zirconia (YSZ) powders was painted to partly cover the oxidized surfaces of the coupons. The YSZ powders were used to prevent the Pt particles from coalescing during high temperature exposure. The thermal expansion of Pt was used for determining the temperature of the oxide layer.

The diffraction data was collected by a GE two-dimensional detector, using 70 keV X-rays focused to a 20 μm high and 200 μm wide rectangle shape.

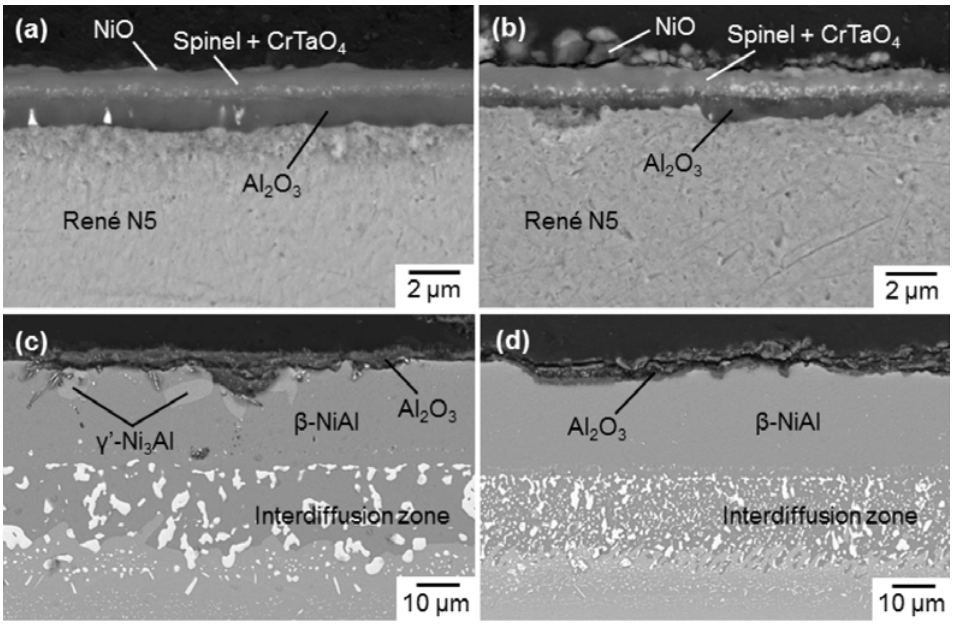

Figure 3. Backscattered electron images of the pre-oxidized specimens: (a) René N5, 1093 °C/68 h, (b) René N5, 982 °C/ 68 h, (c) vapor phase aluminide coating, 1093 °C/68 h, (d) vapor phase aluminide coating, 982 °C/ 68 h.

The beam center and detector distortion were determined using unstrained ceria powder diffraction pattern. In-plane strain was obtained from the elliptical distortion of the diffraction rings using $\sin^2\psi$ method [6,12,15]. The elliptical distortion, D, is

$$D = (d_{\psi=0^o} - d_{\psi=90^o})/d_{\psi=0^o}. \quad (1)$$

Where $d_{\psi=0^o}$ is the in-plane lattice spacing and $d_{\psi=90^o}$ is the out-of-plane lattice spacing for a given (hkl). The sign of this quantity identifies a tensile $(+)$ and compressive $(-)$ condition. Quantities of $d_{\psi=0^o}$ and $d_{\psi=90^o}$ were obtained by fitting diffraction ring of α-Al_2O_3 (116) based on the 2D diffraction formulas by He *et al.* [17] using the MATLAB program by Almer *et al.* [12]. Among the α-Al_2O_3 reflections, the (116) reflection was chosen, because it is a high order reflection with a relatively high intensity and no overlap with reflections from other oxides. To quantify the in-plane strain state ε_{11}, it was assumed that the oxide is an isotropic distribution of crystallites in a biaxially stressed film with no shear based on the observation of the diffraction rings showing absence of strong texture in the α-Al_2O_3 layer (Sect. 3.2.1).

For this case, it can be shown that

$$\varepsilon_{11} \approx D(1-\nu)/(1+\nu) \quad (2)$$

where ν is Poisson's ratio, and that the stress σ_{11} is

$$\sigma_{11} \approx E\varepsilon_{11}/(1-\nu) \quad (3)$$

where E is Young's modulus.

Table 1 shows Young's modulus, E, and Poisson's ratio, ν, of α-Al_2O_3 at the room temperature, 982 °C, 1093 °C used for the strain and stress calculations. Based on our assessment of literature data, the values measured by Sakaguchi *et al.* [18] and Fukuhara *et al.* [19] using pure bulk α-Al_2O_3 were selected.

Table 1. Young's modulus and Poisson's ratio of α-Al_2O_3 used for the strain and stress calculations.

Temperature	Young's modulus (GPa)	Poisson's ratio
Room temperature	380	0.24
982 °C	330	0.25
1093 °C	322	0.25

3. Results and discussions

3.1. Oxide structure

The backscattered electron images of the oxide layers formed on the bare René N5 single-crystal superalloy and the vapor phase aluminde coating specimens after the exposure for 68 hours at 1093 °C and 982 °C are shown in Fig. 3.

At both temperatures, the René N5 specimen formed three layers of oxides: a NiO external layer, a spinel ($Ni(Al,Cr)_2O_4$) layer where fine particles of $CrTaO_4$ were embedded, and an α-Al_2O_3 layer adjacent to the superalloy substrate. The thickness of the α-Al_2O_3 layer was about 1 μm after the exposure at 1093 °C, and about 0.5 μm after the exposure at 982 °C. The thickness of the spinel layer was about 1 μm at both temperatures.

The vapor phase aluminide coating specimens formed a layer of α-Al_2O_3 after the exposure at 1093 °C and 982 °C. The thickness was about 3 μm. In the coupon oxidized at 1093 °C, formation of γ'-Ni_3Al phase was observed beneath the α-Al_2O_3 layer due to the consumption of Al.

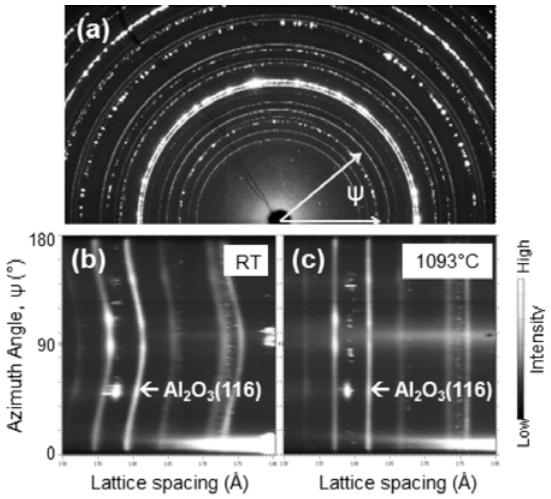

Figure 4. (a) Diffraction rings obtained from the René N5 specimen pre-oxidized at 1093 °C, and the lattice spacing at (b) room temperature and (c) 1093 °C.

Table 2. Room temperature in-plane stresses and strains of the α-Al_2O_3.

Material	Pre-oxidation temperature (°C)	In-plane stress, σ_{11} (GPa)	In-plane strain, ε_{11} (%)
René N5	1093	−4.95	−0.99
	982	−3.87	−0.77
Vapor phase aluminde	1093	−2.71	−0.54
	982	−2.70	−0.54

3.2. Oxide growth strains

3.2.1. Oxide growth strains at room temperature

An example of diffraction rings obtained from the oxide layer of the René N5 specimen pre-oxidized at 1093 °C is shown in Fig. 4a. Figure 4b shows the lattice spacing as a function of azimuth angle. Since the specimen was pre-oxidized at elevated temperature, the diffraction rings exhibited significant strains at room temperature due to the contraction of the superalloy. The lattice spacing of the α-Al_2O_3 was smaller at 0 and 180° than at 90 °, which indicates that there is an in-plane compressive strain in the α-Al_2O_3 layer. Using a MATLAB code [12,17], $d_{\psi=90^o}$ and $d_{\psi=0^o}$ of the Al_2O_3 (116) reflection were determined, and ε_{11} and σ_{11} were calculated using the Eqs. (1)–(3). The intensities of the α-Al_2O_3 diffraction rings are relatively constant from 0 to 180° (Figs. 4a–c), which indicates that the α-Al_2O_3 layer does not have strong grain texture. Table 2 shows the room temperature in-plane stresses and strains in the α-Al_2O_3 layer formed on the René N5 and the vapor phase aluminde coating specimens. All specimens exhibited large in-plane compressive strains up to 1%. The René N5 specimen pre-oxidized at 1093 °C exhibited a larger compressive in-plane strain than at 982 °C. The vapor phase aluminide specimens had almost same strains regardless of the pre-oxidation temperatures.

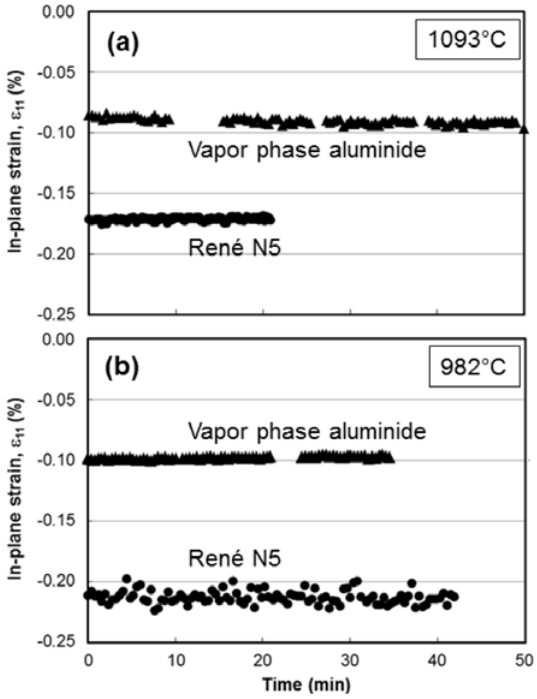

Figure 5. In-plane growth strains of the α-Al2O3 formed on René N5 and vapor phase aluminide showing consistent strains during measurement duration at (a) 1093 °C and (b) 982 °C.

3.2.2. In-situ oxide growth strain measurements

Figure 4c shows the lattice spacing plot of the same specimen obtained after heating to 1093 °C. The lattice spacing of the α-Al_2O_3 (116) peak showed little dependency on azimuth angle. However, using the same diffraction peak analysis algorithm, it was confirmed that there was a small in-plane compressive stress and strain. Figure 5 shows the in-plane strains of the α-Al_2O_3 layer on the René N5 and the vapor phase aluminide coating specimens during the measurements at 1093 °C (Fig. 5a) and 982 °C (Fig. 5b). During the measurements, the oxide growth strains were consistent over the time. These results indicate that strain accumulation due to oxide growth and strain relaxation due to creep are in near equilibrium condition after the pre-oxidation for 68 hours. Table 3 summarises the *in-situ* measurement results. The α-Al_2O_3 had larger in-plane compressive strains on the René N5 specimens compared with the vapor phase aluminide specimens at both temperatures. The oxide growth strain on the René N5 was higher at 982 °C than at 1093 °C. On the other hand, the oxide growth strain on the vapor phase aluminde specimen did not show temperature dependency.

The dominant source of potential error to the measured strain value is temperature uncertainty. The temperature uncertainty can cause thermal expansion or contraction of the superalloy substrate, which can be as much as 0.02% strain. The errors from the strain analysis of the 2D diffraction patterns [12,17] are less than 0.01%, which is much smaller than that from temperature uncertainty.

Table 3. *In-situ* in-plane stress and strain of the α-Al_2O_3 layer.

Material	Temperature (°C)	In-plane stress, σ_{11} (GPa)	In-plane strain, ε_{11} (%)
René N5	1093 °C	−0.75	−0.17
	982 °C	−0.94	−0.21
Vapor phase aluminde	1093 °C	−0.40	−0.09
	982 °C	−0.43	−0.10

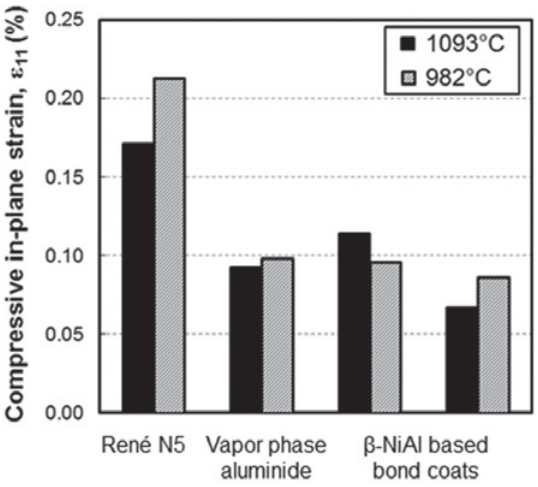

Figure 6. Comparison of the compressive in-plane strains of the α-Al_2O_3 layer formed on René N5 single-crystal superalloy and three β-NiAl based bond coats.

3.2.3. Oxide growth strains on β-NiAl bond coats

The same *in-situ* oxide growth strain measurement approach was applied to two different β-NiAl based industrial bond coats. Figure6 shows a comparison of the in-plane compressive strains of the α-Al_2O_3 layers. The strains measured on three different β-NiAl based bond coats were consistently smaller than the ones on René N5, and roughly at −0.1%, independent of both bond coat chemistry and temperature. Smaller in-plane compressive oxide growth strains are expected to be beneficial in suppressing both bond coat rumpling and oxide-assisted crack growth. However, the obtained results indicate that it may be difficult to reduce the compressive oxide growth strains on the β-NiAl based bond coats by modifying bond coat chemistry. Exploration of different bond coat systems outside the β-NiAl based compositions may be required to identify an alternate path to improve crack growth resistance of the bond coat materials.

4. Summary

In-situ measurements of the growth strains of the α-Al_2O_3 layers formed on the single-crystal superalloy and the β-NiAl based bond coats were performed using high energy synchrotron X-rays. The followings were observed:

(1) At elevated temperatures, the in-plane growth strains of the α-Al_2O_3 were compressive in both René N5 superalloy and vapor phase aluminide bond coat specimens.
(2) The in-plane compressive growth strains of the α-Al_2O_3 formed on the β-NiAl based bond coats were smaller than those on the superalloy specimen, and independent of bond coat chemistry and temperature.

The authors are thankful to S.J. Duclos, M.L. Blohm, PR Subramanian for their program support. J.R. Cournoyer, E.H. Hearn of GE Global Research, and Ali Mashayekhi and Roger Ranay at Sector 1 of APS are greatly acknowledged for their technical support.

Use of the Advanced Photon Source, an Office of Science User Facility operated for the U.S. Department of Energy (DOE) Office of Science by Argonne National Laboratory, was supported by the U.S. DOE under Contract No. DE-AC02-06CH11357.

References

[1] A. Suzuki, M.F.X. Gigliotti, B.T. Hazel, D.G. Konitzer, T.M. Pollock, Metall. Mater. Trans. A, **41A**, 947 (2010)
[2] A.G. Evans, D.R. Mumm, J.W. Hutchinson, G.H. Meier, F.S. Pettit, Prog. Mater. Sci., **46**, 505 (2001)
[3] A.G. Evans, M.Y. He, A. Suzuki, M. Gigliotti, B. Hazel, T.M. Pollock, Acta Mater., **57**, 2969 (2009)
[4] M.Y. He, A.G. Evans, Acta Mater., **58**, 583 (2010)
[5] T.M. Pollock, B. Laux, C.L. Brundidge, A. Suzuki, M.Y. He, J. Am. Ceram, Soc., **94**, S136 (2011)
[6] B.W. Veal, A.P. Paulikas, P.Y. Hou, Nature Materials, **5**, 349 (2006)
[7] B.W. Veal, A.P. Paulikas, R.C. Birtcher, Appl. Phys. Lett., **89**, 161916 (2006)
[8] P.Y. Hou, A.P. Paulikas, B.W. Veal, Mat. Sci. Forum, **522-523**, 433 (2006)
[9] B.W. Veal, A.P. Paulikas, P.Y. Hou, Appl. Phys. Lett., **90**, 121914 (2007)
[10] B.W. Veal, A.P. Paulikas, B. Gleeson, P.Y. Hou, Surf. Coat. Tech., **202**, 608 (2007)
[11] B.W. Veal, A.P. Paulikas, J. Appl. Phys., **104**, 093525 (2008)
[12] J.D. Almer, G.A. Swift, J.A. Nychka, E. Üstündag, D.R. Clarke, Mat. Sci. Forum, **490-491**, 287 (2005)
[13] B. Laux, T.M. Pollock (to be published)
[14] T.M. Pollock, D.M. Lipkin, K.J. Hemker: MRS Bulletin, **37**, 923 (2012)
[15] I.C. Noyen, J.B. Cohen, Residual Stress Measurement by Diffraction and Interpretation (Springer, New York, 1987)
[16] B.B. He, Two-dimensional X-ray Diffraction (Wiley, New Jersey, 2009)
[17] S. Sakaguchi, N. Murayama, Y. Kodama, F. Wakai, J. Mat. Sci. Lett., **10**, 282 (1991)
[18] M. Fukuhara, I. Yamauchi, J. Mat. Sci., **28**, 4681 (1993)